The atomic weight of cerium, 140.12, was taken from Cameron and Wichers (*1*).

DISCUSSION

Values are tabulated to the nearest 0.0001 cal. deg.$^{-1}$ mole^{-1} in order to facilitate rounding to three decimal places. Uncertainties in the multiplicities of 21 of the higher energy levels result in an uncertainty of 0.0034 cal. deg.$^{-1}$ mole^{-1} in the Gibbs energy function and 30 cal. mole^{-1} in the heat content at 6000° K. This uncertainty becomes insignificant below about 1500° K.

By comparing with the tabulated values, the results obtained when the 47 energy levels between 19,000 and 20,000 cm.$^{-1}$ were omitted, it was found that omission of the levels introduced a lowering of 3% in $Cp°$ at 6000° K., and less at lower temperatures. The possibly 30 missing levels below 20,000 cm.$^{-1}$ should have less effect than this. The present values differ significantly from those calculated by Feber and Herrick because of the contributions of the many higher levels unavailable to them.

ACKNOWLEDGMENT

We are indebted to W. C. Martin for supplying us with his unpublished energy level data from work in progress and to Ralph Hultgren for helpful assistance.

LITERATURE CITED

(1) Cameron, A.E., Wichers, E., *J. Am. Chem. Soc.* **84**, 4175-97 (1962).
(2) Feber, R.C., Herrick, C.C., U.S. Atomic Energy Commission Rept. **LA-3184** (1965).
(3) Lewis, G.N., Randall, M., Pitzer, K.S., Brewer, L., "Thermodynamics," 2nd ed., pp. 419-24, McGraw-Hill, New York, 1961.
(4) Martin, W.C., private communication.
(5) National Bureau of Standards, *Tech. News Bull.* **47**(10), 175-7 (1963).

RECEIVED for review January 29, 1968. Accepted May 25, 1968. Work supported by the U. S. Atomic Energy Commission.

Particle Size Distribution in Compacts of Solids

Y. B. G. VARMA, T. GOPICHAND, and D. VENKATESWARLU
Indian Institute of Technology, Madras 36, India

Knowledge of particle size distribution in compacts is useful in studies of porous beds and catalysts. Compacts of 2 cm. diameter of calcite, sand, quartz, barytes, marble, and soapstone in the initial particle size range of −0.200, +0.125 to −0.050, +0.040 cm. are prepared by application of pressures of 93 to 3153 kg. per sq. cm. and disintegrated into individual particles by acetone. The sizes of the disintegrated particles are determined by sieve analysis. The particle size distributions are given using a modified upper limit equation. The standard deviation is characteristic of the material. An equation relating mean diameter of size distribution to the initial particle size and surface energy of material, diameter of compact, and pressure of compaction is presented on the basis of dimensional analysis and experimental data.

COMPACTION is a technique of size enlargement of small particles of materials by compressing them into a coherent mass. It is used extensively for briquetting peats, lignites, and bituminous coals, tableting of pharmaceuticals, compacting metal powders, and pelleting of catalysts. The most important macroscopic characteristic of compacts which has been studied is porosity (*1, 4, 5, 7, 10*).

From the results of an experimental study of porosities of compacts of six materials of different initial particle sizes compacted at the pressures given in Table I, the porosity of compacts is correlated (*10*) by

$$\epsilon\epsilon_0^2 = k\left(\frac{\nu}{Pd_{\text{av}}}\right)^m \tag{1}$$

The exponent m is equal to 0.1 of the coefficient of internal friction (Table II), but the porosity data do not give an idea about the size distribution of particles within the compact, which is necessary in studies of porous beds and catalysts, as compacts of same porosity may have different surface areas. This study, which seems to be the first of its kind reported, relates the size distribution to the physical properties of material and the conditions of compaction.

The particles from which the compact is made may be presumed to be subjected to certain basic processes, resulting in particle disintegration and size distribution within the compact. Under small loads, the particles may be pushed into the void spaces, causing consolidation which may progress until the individual void size is less than the particle size. As the load increases, the particles bearing the load may yield and the resulting smaller particles may fill the void spaces. This process may continue until the applied load is balanced by the bearing capacity of the particles. However, the actual compaction process may be complicated by the shape and orientation of the particles and simultaneous occurrence of consolidation and disintegration. These observations are for brittle materials. For plastic materials, these processes are further complicated since the voidage may also be reduced owing to plastic deformation and subsequent fusion of the particles.

The literature on particle size distributions within compacts is limited and most references deal with the types of packings of regular and irregular shaped particles of

Table I. Initial Particle Sizes and Compaction Pressure Data

Material	Initial Particle Sizes, Cm.	Compaction Pressures, Kg./Cm.^{2}	Range of Porosities
Calcite	−0.200, +0.125; −0.125, +0.100; −0.100, +0.080; −0.080, +0.050; −0.050, +0.040	94, 188, 282, 422, 751, 1455, and 2394	15.12 to 41.00
Sand	−0.100, +0.080; −0.080, +0.050; −0.050, +0.040	315, 473, 788, 1577, 2365, and 3153	16.84 to 40.05
Quartz	−0.200, +0.125; −0.125, +0.100; −0.100, +0.080; −0.050, +0.040	158, 315, 473, 788, 1577, 2365, and 3153	16.70 to 42.58
Barytes	−0.200, +0.125; −0.125, +0.100; −0.100, +0.080; −0.050, +0.040	93, 232, 395, 744, 1441, and 2370	13.27 to 34.96
Marble	−0.200, +0.125; −0.125, +0.100; −0.100, +0.080	93, 232, 395, 744, 1441, and 2600	18.26 to 38.37
Soapstone	−0.200, +0.125; −0.125, +0.100; −0.100, +0.080; −0.050, +0.040	93, 232, 395, 744, 1441, and 2370	8.87 to 29.55

Table II. Relationship of *m* to Internal Friction

Material	Angle of Internal Friction, ϕ°	tan ϕ	*m*
Calcite	70–71	2.75–2.90	0.28
Sand	71–72	2.90–3.10	0.30
Quartz	70–71	2.75–2.90	0.28
Barytes	70–71	2.75–2.90	0.28
Marble	60–61	1.73–1.80	0.18
Soapstone	72–73	3.10–3.30	0.33

loose beds (*2, 3*). Turba and Rumpf (*8*) reported the particle size distributions in compacts of thermally crushed barytes of 50- to 100-micron initial size range and presented the distributions on Rosin-Rammler-Sperling (RRS) probability charts for coarse range and on arithmetic probability charts for finer ranges.

EXPERIMENTAL

Compaction of materials is carried out in a 200,000-pound laboratory hydraulic press fitted with an 8-inch diameter Bourdon-type pressure gage calibrated to an accuracy of 1% of the indicated load. The die set consists of bottom plate, bottom punches, die, plungers, and top plate for making six compacts of 2-cm. diameter at a time. Weighed equal quantities of each particle size range of materials are taken into the six die holes and a load is applied gradually at a constant rate until the required pressure is reached. The load is maintained constant for 120 seconds, and after releasing the load, the compacts are ejected out of the die and the porosity is calculated (*2*).

Particle size distribution in compacts is determined after disintegrating the compact into its constituent particles using acetone. A number of preliminary experiments have been carried out to ensure that the constituent particles are not broken by acetone and that results are reproducible. Size ranges of constituent particles are determined by standard sieves.

RESULTS

Typical plots of particle size *vs.* cumulative percentages of particles retained on normal probability charts for different initial size ranges for calcite, sand, quartz, barytes, marble, and soapstone are given in Figure 1. The following observations are made from the data and plots: Size reduction of the initial particles occurs during compaction.

The particle size distribution lines in each figure—i.e., for a material of a given initial particle size compacted at different pressures—have the same general pattern. Therefore, the pattern of size distribution on application of pressure seems to be the same for a given particle size of a material and to be independent of compaction pressure, in the range of pressures investigated.

Compacts of different materials made from the same initial particle sizes and pressure show different size distributions.

Particle size distribution data of disintegrated compacts is also plotted as other functions (square and square root of particle size *vs.* cumulative percentage on normal and logarithmic probability charts), but these are not useful for correlating the data.

The particles in compacts do not have normal distribution. This is because there cannot be particles bigger than the initial particles taken, which limits the distribution. A similar situation involving upper limit of size distribution occurs in atomization of liquids through nozzles. Mugele and Evans (*6*) suggest the use of upper limit equation given below for the size distribution of droplets:

$$f(x) = \frac{1}{\sigma_g x \left[2\pi\right]^{1/2}}\, e^{-\ln\left(\frac{x_\infty - x}{x_g}\right)^{2}/(2\sigma_g^2)} \qquad (2)$$

The authors plot the data as $d/(d_{\max} - d)$ *vs.* cumulative percentages on logarithmic probability plots. The value of $d_{\max}$ in this equation is determined either by trial and error or from the trend of the distribution by plotting diameter of particles *vs.* cumulative percentage and reading the 10th, 50th, and 90th percentiles, d_{10}, d_{50}, and d_{90}. $d_{\max}$ is then given by the equation:

$$d_{\max} = d_{50}\left[\frac{d_{50}(d_{90} + d_{10}) - 2d_{90}d_{10}}{d_{50}^2 - d_{90}d_{10}}\right] \qquad (3)$$

The use of this equation is limited as it requires prior knowledge of particle size distribution.

Typical particle size distributions of compacts of materials plotted as $d/(d_{\max} - d)$ *vs.* cumulative percentages of particles retained on logarithmic probability plots are shown in Figure 2. $d_{\max}$ is taken as the maximum particle size in the initial size range—i.e., for an initial size range of −0.200, +0.125 cm., $d_{\max}$ is taken as 0.200 cm. The values of $d/(d_{\max} - d)$ are calculated by taking d as the minimum size in the particle size range—i.e., for a particle size range of −0.200, +0.125 cm., the value of $d/(d_{\max} - d)$ is calculated as 0.125/(0.200 − 0.125) or 1.667. The following observations are made from the plots: The size distribution data of a material of a specific particle size may be represented for each compaction pressure by a straight line. The initial particle sizes are, however, displaced from this line. This shows that only the particles which are reduced in size during compaction follow the straight line distribution and the original uncrushed particles do not follow this distribution pattern.

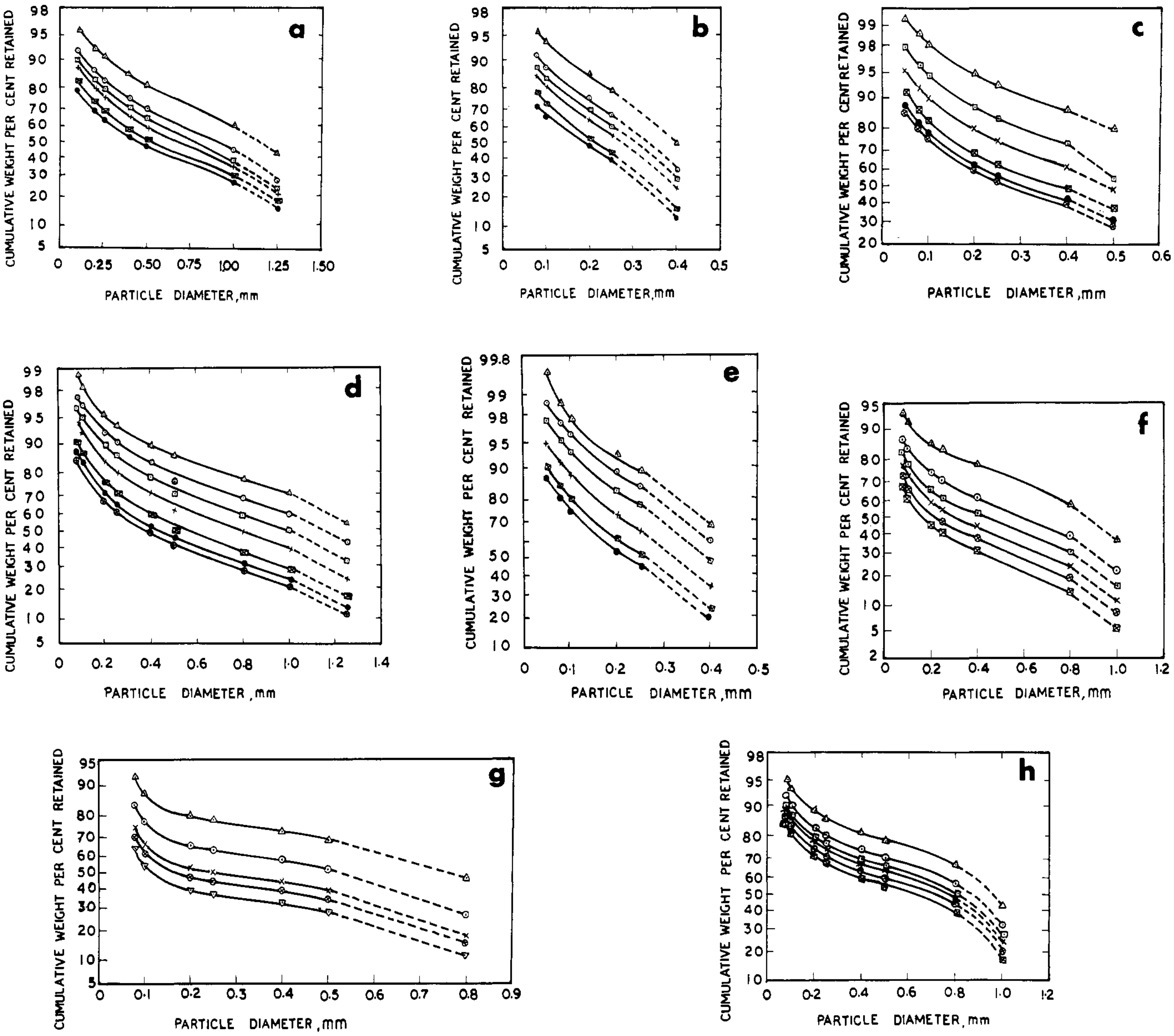

Figure 1. Plot of particle diameter *vs.* cumulative weight per cent retained

			△	⊙	⊡	×	⊠	●	⊗
a. Calcite,	−2.00, +1.25 mm.	*P*	94	188	282	422	751	1455	
		ϵ	36.42	30.50	26.79	24.54	21.97	17.38	
b. Calcite,	−0.50, +0.40 mm.	*P*	94	188	282	422	751	1455	
		ϵ	41.00	36.65	32.68	30.07	26.48	21.33	
c. Sand,	−0.80, +0.50 mm.	*P*	315	473	788	1577	2365	3153	
		ϵ	38.00	32.92	28.39	22.88	19.44	17.60	
d. Quartz,	−2.00, +1.25 mm.	*P*	158	315	473	788	1577	2365	3153
		ϵ	35.31	32.17	28.92	24.06	19.96	17.73	16.70
e. Quartz,	−0.50, +0.40 mm.	*P*	158	315	473	788	1577	2365	
		ϵ	42.58	39.87	36.15	30.86	25.50	22.74	
f. Barytes,	−1.25, +1.00 mm.	*P*	93	232	395	744	1441	2370	
		ϵ	33.60	26.30	22.97	19.90	16.17	13.49	
g. Marble,	−1.00, +0.80 mm.	*P*	93	232	744	1441	2600		
		ϵ	38.37	31.00	25.26	22.65	20.57		
h. Soapstone,	−1.25, +1.00 mm.	*P*	93	232	395	744	1441	2370	
		ϵ	28.47	20.16	16.21	13.13	10.82	9.25	

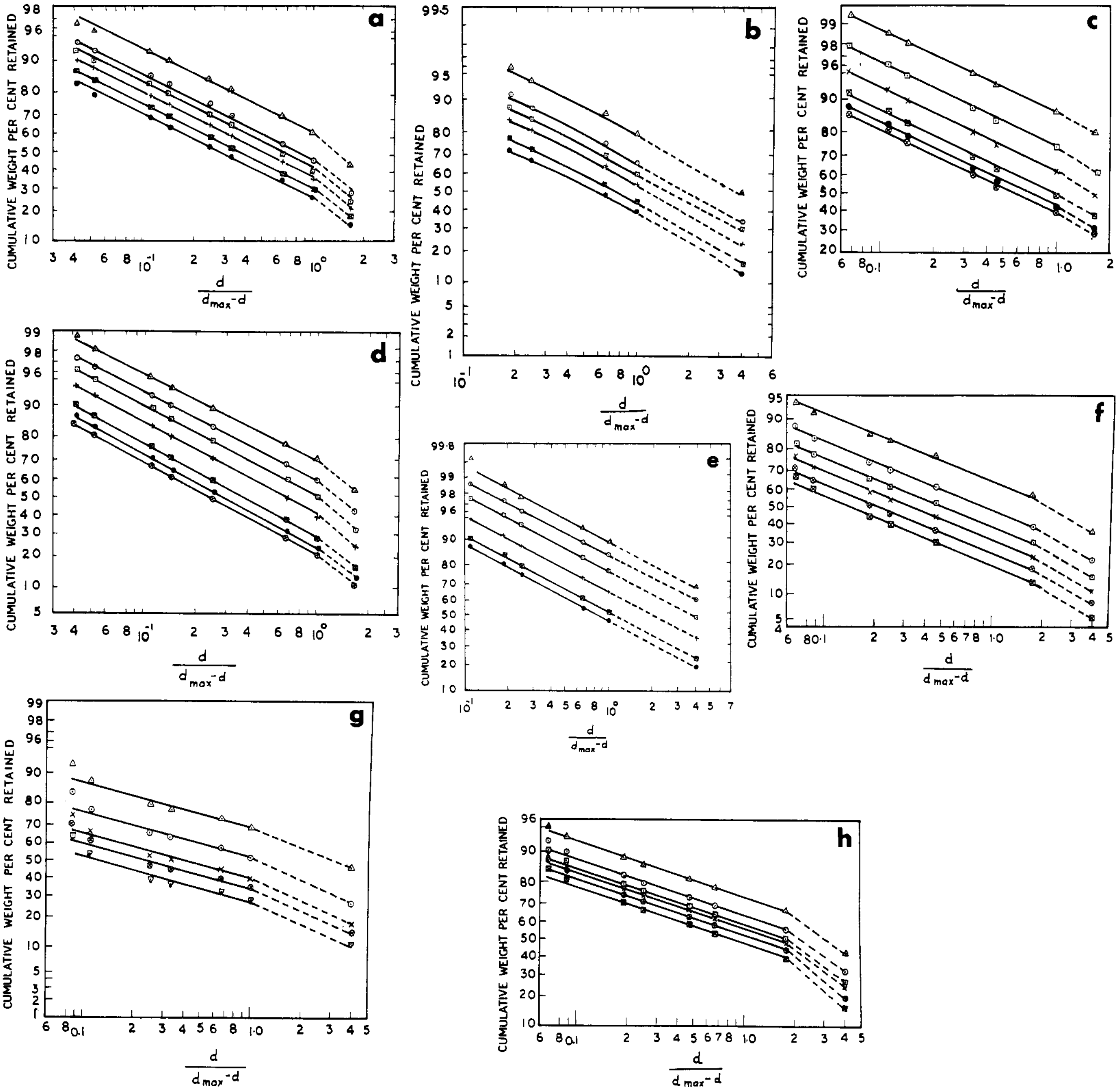

Figure 2. Plot of $d/(d_{max} - d)$ vs. cumulative weight per cent retained

			△	⊙	⊡	×	⊠	●	⊗
a. Calcite,	−2.00, +1.25 mm.	P	94	188	282	422	751	1455	
		ϵ	36.42	30.50	26.79	24.54	21.97	17.38	
b. Calcite,	−0.50, +0.40 mm.	P	94	188	282	422	751	1455	
		ϵ	41.00	36.65	32.68	30.07	26.48	21.33	
c. Sand,	−0.80, +0.50 mm.	P	315	473	788	1577	2365	3153	
		ϵ	38.00	32.92	28.39	22.88	19.44	17.60	
d. Quartz,	−2.00, +1.25 mm.	P	158	315	473	788	1577	2365	3153
		ϵ	35.31	32.17	28.92	24.06	19.96	17.73	16.70
e. Quartz,	−0.50, +0.40 mm.	P	158	315	473	788	1577	2365	
		ϵ	42.58	39.87	36.15	30.86	25.50	22.74	
f. Barytes,	−1.25, +1.00 mm.	P	93	232	395	744	1441	2370	
		ϵ	33.60	26.30	22.97	19.90	16.17	13.49	
g. Marble,	−1.00, +0.80 mm.	P	93	232	744	1441	2600		
		ϵ	38.37	31.00	25.26	22.65	20.57		
h. Soapstone,	−1.25, +1.00 mm.	P	93	232	395	744	1441	2370	
		ϵ	28.47	20.16	16.21	13.13	10.82	9.25	

All the lines of a specific particle size for different pressures are parallel, and hence, the standard deviation, σ_g, is independent of compaction pressure.

The lines are also parallel to each other for particles of different sizes of same material, and hence, the standard deviation, σ_g, is independent of initial particle size d_{av}.

The value $d/(d_{max} - d)$ corresponding to 50% cumulative weight of particles varies with initial particle size and compaction pressure.

The standard deviation, σ_g, is calculated from the relation

$$\sigma_g = \log \frac{\left[\dfrac{d}{d_{max} - d}\right]_{84.13}}{\left[\dfrac{d}{d_{max} - d}\right]_{50}} \qquad (4)$$

Table III gives the range of σ_g values calculated by Equation 4. σ_g is fairly constant and seems to be characteristic of a material.

By dimensional analysis, it can be shown that

$$\left[\frac{d_m}{d_{av}}\right] = K\left[\frac{\nu}{Pd_{av}}\right]^p \left[\frac{d_{av}}{D}\right]^q \qquad (5)$$

The surface energy values in kilogram centimeter per square centimeter are 0.311, 0.745, 0.753, 0.200, 0.216, and 0.452 for calcite, sand, quartz, barytes, marble, and soapstone, respectively, (*9*). From plots of cumulative weight per cent retained *vs.* $d/(d_{max} - d)$ such as Figure 2 for calcite, the value of $d/(d_{max} - d)$ for 50% is read. The value of d calculated from the known value of $d/(d_{max} - d)$ gives the mean diameter d_m corresponding to a known value of d_{max}. The average diameter, d_{av}, is the arithmetic average of the sieve range—i.e., for a particle size range of −0.200, +0.125 cm., the average diameter, d_{av}, is 0.1625 cm. The diameter, D, is the actual diameter of the cylindrical compact as measured by calipers. Figure 3 is a plot of (d_m/d_{av}) *vs.* $(\nu/Pd_{av})^p(d_{av}/D)^q$ for all the materials investigated. The values of p and q which represent the data of each material by a single line of slope 1 are given in Table IV.

The correlations and figures presented indicate a method of predicting particle size distribution in compacts. The particle size distribution of compacts of a material of a specific particle size compacted at different pressures may be predicted from the data of two compaction tests. The following steps may be followed for this: Draw two lines of $d/(d_{max} - d)$ *vs.* cumulative weight percentages on logarithmic probability plots for a sample of a given particle size range at the two compaction pressures investigated. Determine the values of d_m and σ_g from the two lines. Calculate (d_m/d_{av}) and (ν/Pd_{av}) for the two compaction pressures studied. Locate these two values on logarithmic coordinates of (d_m/d_{av}) *vs.* (ν/Pd_{av}). Draw a straight line

Table III. Range of σ_g Values

Material	Std. Dev.
Calcite	0.82–0.89
Sand	0.79–0.90
Quartz	0.72–0.85
Barytes	0.89–1.10
Marble	1.18–1.60
Soapstone	1.12–1.24

Table IV. p and q Data

Material	p	q
Calcite	0.35	0.00
Sand	0.42	0.00
Quartz	0.43	0.00
Barytes	0.55	0.18
Marble	0.58	0.79
Soapstone	0.17	0.00

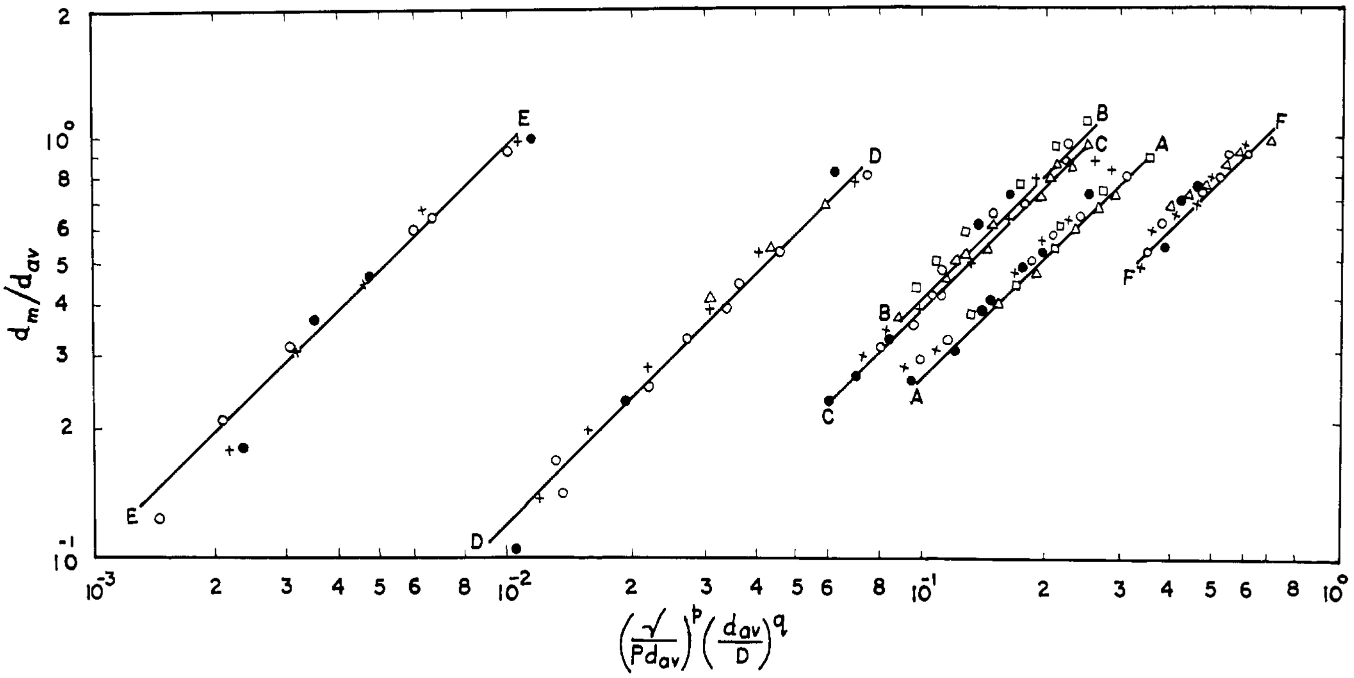

Figure 3. Plot of (d_m/d_{av}) *vs.* $(\nu/Pd_{av})^p(d_{av}/D)^q$

AA	Calcite	● −2.00, +1.25 mm.
BB	Sand	× −1.25, +1.00 mm.
CC	Quartz	○ −1.00, +0.80 mm.
DD	Barytes	□ −0.80, +0.50 mm.
EE	Marble	△ −0.50, +0.40 mm.
FF	Soapstone	

Table V. Calculated Values of Compaction Data

Particle Size	Compaction Pressure, Kg./Cm.^{2}	d_m	σ_g	d_m/d_{av}	ν/Pd_{av}	d_{av}/D	$(\nu/Pd_{av})^p (d_{av}/D)^q$
–0.200, +0.125	751	0.0519	0.82	0.319	2.549×10^{-3}	8.025×10^{-2}	0.12
	422	0.0667	0.82	0.410	4.535×10^{-3}	8.025×10^{-2}	0.15
–0.050, +0.040	282	0.0315	0.82	0.700	2.451×10^{-3}	2.23×10^{-2}	0.27

through these points. Read (d_m/d_{av}) values for required pressures from this line by interpolation or extrapolation.

Using d_m and σ_g values, construct distribution lines for any required compaction pressures for the material of the given initial particle size.

Similarly, the particle size distributions of compacts of a material of different particle sizes made at different pressures may be predicted if data of one more particle size at any one pressure is available. The procedure for this is as follows: Cumulative probability lines as shown in Figure 2 are drawn using the experimental values. From these lines, d_m and σ_g values are determined.

Corresponding values of (d_m/d_{av}), (ν/Pd_{av}) and (d_{av}/D) are calculated.

Using these three sets of points, (d_m/d_{av}) *vs.* $(\nu/Pd_{av})^p(d_{av}/D)^q$ is plotted as shown in Figure 3 choosing appropriate values of p and q such that the three points fall in a straight line of slope 1.

For example, if the experimental data of calcite of size range –0.200, +0.125 cm. compacted at 751 and 422 kg. per sq. cm. and of size range –0.050, +0.040 cm. compacted at 282 kg. per sq. cm., are as given in columns 3 and 4 of Table V, the values given in columns 5 to 8 may be calculated as indicated above.

From these values, line *AA* of Figure 3 may be drawn and the particle size distribution for any initial particle size of calcite compacted at any pressure may be predicted.

NOMENCLATURE

D = diameter of compact, cm.
d = diameter of particle, cm.
d_{av} = average diameter of particle, cm.
d_{max} = maximum diameter of particle that exists in the compact, cm.
d_m = mean diameter of particles calculated from 50% value of the distribution, cm.
K = coefficient in Equation 5
k = coefficient in Equation 1
m = exponent in Equation 1
P = compaction pressure, kg./sq. cm.
p,q = exponents in Equation 5
x = distributed factor
x_m = maximum value of the distributed factor
x_n = mean value of the distributed factor
ϵ = porosity of the compact, dimensionless
ϵ_0 = porosity of the uncompacted material just prior to compaction, dimensionless
σ_g = standard deviation
ν = surface energy of material, kg.cm./sq. cm.

LITERATURE CITED

(1) Cooper, A.R., Eaton, L.E., *J. Am. Ceram. Soc.* **45**, No. 3, 97 (1962).
(2) Dallavalle, J.M., "Micromeritics," 2nd ed., pp. 123, 131, Pitman, New York, 1948.
(3) Deresiewicz, H., "Mechanics of Granular Matter" in "Advances in Applied Mechanics," H.L. Dryden, Th.Von. Karman, Eds., 1st ed., Vol. **5**, pp. 237, Academic Press, New York, 1958.
(4) Huffine, Coy L., Bonilla, C.F., *A.I.Ch.E. J.* 8, No. 4, 490 (1962).
(5) Komarek, K.R., 7th Biennial Conf. Intern. Briquetting Assoc., Jackson, Wyo., **48** (1961).
(6) Mugele, R.A., Evans, H.D., *Ind. Eng. Chem.* **43**, No. 6, 1317 (1951).
(7) Train, D., *J. Pharm. (London)* **8**, 745 (1956).
(8) Turba, E., Rumpf, H., *Chem. Ing.-Tech.* **36**, 230 (1964).
(9) Varma, Y.B.G., Ramani, A.V., Venkateswarlu, D., *J. Chem. Eng. Soc. I.I.T. Madras* **1**, 1 (1967).
(10) Varma, Y.B.G., Venkateswarlu, D., *Chem. Process Eng.* **48**, No. 7, 77 (1967).

RECEIVED for review November 28, 1966. Resubmitted June 23, 1967. Accepted February 28, 1968.